

AISC 2005 코드를 활용한 콘크리트 충전 합성기둥의 해석과 평가

박지웅¹ · 이두재² · 장성수³ · 허종완⁴

인천대학교 건설환경공학과 석사과정¹, 대림산업 차장², (주) 콘프라 대표이사³,
인천대학교 건설환경공학과 교수, 교신저자⁴

Advanced Analysis of Connections to Concrete-Filled Steel Tube Columns using the 2005 AISC Specification

Park, Ji-Woong¹ · Rhee, Doo-Jae² · Chang, Suong-Su³ · Hu, Jong-Wan⁴

¹Dept. of Civil and Environmental Engineering, University of Incheon, The Masters Course (Student Member)

²Daelim Industrial Co.Ltd. Duputy Department Head

³CONFRA Co.Ltd. President

⁴Dept. of Civil and Environmental Engineering, University of Incheon (Member)

Abstract: Concrete filled steel tube (CFT) columns have been widely used in moment resisting frame structures both in seismic zones. This paper discusses the design of such members based on the advanced methods introduced in the 2005 AISC Specification and the 2005 Seismic Provisions. This study focuses particularly on design following both linear and nonlinear methods utilizing equivalent static and dynamic loads for low-rise moment frames. The paper begins with an examination of the significance of pseudo-elastic design interaction equations and the plastic ductility demand ratios due to combined axial compressive force and bending moment in CFT members. Based on advanced computational simulations for a series of five-story composite moment frames, this paper then investigates both building performance and new techniques to evaluate building damage during a strong earthquake. It is shown that 2D equivalent static analyses can provide good design approximations to the force distributions in moment frames subjected to large inelastic lateral loads. Dynamic analyses utilizing strong ground motions generally produce higher strength ratios than those from equivalent static analyses, but on more localized basis. In addition, ductility ratios obtained from the nonlinear dynamic analysis are sufficient to detect which CFT columns undergo significant deformations.

Key Words: Concrete filled tubes, CFT, interaction ratio, dynamic loads, ductility, moment resisting frames.

1. Introduction

In the last two decades, concrete filled steel tubes (CFTs) have received widespread acceptance in many parts of the world, particularly in Japan and other countries in Southeast Asia. CFTs are used as columns in multistory buildings as well as bridge piers because of their superior ductility and toughness. These outstanding

performance characteristics are associated with the synergetic action of its ductile steel and high compressive strength concrete components (Roeder, 2000). Some of the advantages of CFT columns over other either steel or reinforced concrete systems include (Azizinamini and schneider, 2011; Hajjar, 2002; Seon and Hu, 2011):

- Use of the stiffening action from the concrete to prevent local buckling of slender steel wall

주요어: 콘크리트 충전 기둥 (CFT), 상호작용 비, 동적하중, 연성, 모멘트 프레임

Corresponding author: Hu, Jong-Wan

Dept. of Civil and Environmental Engineering, University of Incheon, 12-1 Songdo-dong, Yeonsu-gu, Incheon 406-840, Korea
Tel: +82-32-835-8463, Fax: +82-32-835-0775, E-mail: jongp24@incheon.ac.kr

투고일: 2012년 8월 1일 / 수정일: 2012년 8월 17일 / 게재확정일: 2012년 8월 31일

elements, permitting the efficient use of thin steel tubes.

- Use of the confining action by the steel walls to increase both the concrete strength (primarily for circular columns or CCFTs) and its ductility (in both CCFTs and rectangular CTFs, or RCFTs).
- Use of the concrete as a heat sink in case of fire, so that the CFT element can be erected without any fire-proofing if minimal reinforcement in the form of bars is incorporated.
- Use of the steel section as the formwork, considerably reducing construction costs and speeding the completion of the building.

Composite CFT columns are especially suited for moment resisting frames in high seismic areas because they (a) have a high strength to weight ratio due to the confinement effect of concrete core, (b) provide excellent monotonic and dynamic resistance under biaxial bending plus axial force, and (c) improve damping behavior (Tsai et al., 2004). Composite CFT frames consisting of steel I girder and either rectangular or circular CFT columns can be classified into fully restrained (FR) frames when welded connections are used or partially restrained (PR) frames when bolted connections are used. For seismic design, which demands the combination of high stiffness and ductility from the structural systems, it has been demonstrated that properly detailed PR composite frames can provide similar or superior seismic behavior to their FR counterparts (Rassati et al., 2004). The improved performance results from a combination of both (a) the decrease in seismic forces stemming from the additional flexibility of the PR connections, (b) the increase in rotational capacity provided by the PR connection components, and (c) the self-limiting forces in the governing tension yielding mechanisms which can be used to delay or prevent brittle failure modes. Although composite PR connections are desirable for frame structures, it is difficult to model the actual PR joint response in the analysis and design process (Green et al., 2004).

Design provisions based on the full plastic behavior of composite members and systems are particularly useful in limit state calculations for both non-seismic and seismic resistant design. The new USA code provisions for composite construction-namely, the *American Institute of*

Steel Construction 2005 Specification for Structural Steel Buildings (AISC Specification, 2005) and the *Seismic Provisions for Structural Steel Buildings* (Seismic Provision, 2005)-present designers with new guidance on the analysis and design of composite columns and frames. The current *AISC Specification* for composite columns are appropriate for predicting the ultimate capacity of CFT beam-columns corresponding based on a simplified full plastic stress distribution. The full plastic interaction diagram for a cross section can be easily generated through exact or piece-wise linear approximations so that any combination of axial load and moment can be easily checked in design. The distribution used is called simplified because the tensile capacity of the concrete, and in particular any tension stiffening effects, are ignored and the materials are assumed to behave in a bilinear elasto-plastic manner.

The *Seismic Provisions, 2005*, in Part II-Composite Structural Steel and Reinforced Concrete Buildings, address four types of composite moment resisting frames: (a) composite partially restrained moment frames (C-PRMF), (b) composite special moment frames (C-SMF), (c) composite intermediate moment frames (C-IMF), and (d) composite ordinary moment frames (C-OMF). The development of such *Seismic Provisions* for the seismic design of composite structural steel and reinforced concrete buildings was begun by the Building Seismic Safety Council (BSSC) (Viest et al., 1997). These *Seismic Provisions* are based upon the 1994 National Earthquake Hazards Program Provisions (FEMA, 1995) and subsequent modifications made in the 1997, 2000, and 2003 NEHRP Provisions and in ASCE 7 (ASCE, 2002).

Part II of the *Seismic Provisions* also refers to steel moment resisting frames as described in Part I, since composite systems are assemblies of steel and concrete components. Steel moment frame provisions reflect performance observed in both the 1994 Northridge and 1995 Kobe earthquakes and the subsequent research conducted by the SAC Joint Venture for the Federal Emergency Management Agency (FEMA). As part of the SAC project, extensive computational simulations were performed on steel moment resisting frames to simulate the brittle fractures observed during the 1994 North ridge earthquake (FEMA, 1995; ASCE, 2002). These analytical

studies developed a platform to investigate effective methods for evaluating the structural damage and predicting the seismic performance of steel-framed buildings. However, there were no analyses conducted on the static/seismic performance and damage evaluation for composite moment frames. In fact, there is comparatively little research in this area for frames designed to USA codes (El-Tawil et al., 1996).

The purpose of this research is two-fold. First, it examines the monotonic and cyclic behavior of CFT beam-columns subjected to combined axial and moment loading in an attempt to estimate both the maximum strength and ductility for doubly-symmetric and axisymmetric composite cross sections. From these studies it can be shown that ultimate capacities for rectangular/circular CFT beam-columns can be estimated with reasonable accuracy using the simplified axial and moment (P-M) interaction formulas provided by *2005 AISC Specification* for composite systems. Second, based on the analytical study of CFT cross-sectional strength and ductility, advanced computational simulations are carried out on a series of five story composite moment resisting frames. The primary aim of this portion of the study is to develop preliminary damage assessment metrics for low-rise, composite frames designed to the *2005 Seismic Provisions* when subjected to large seismic loads.

2. Methodology

The case studies in this paper comprise both element (composite CFT cross section) analyses and frame analyses. The numerical experiments are performed using a nonlinear structural analysis program, OPENSEES v.1.7.2 (Mazzoni et al., 2005). The cross-sectional analyses include both circular and rectangular concrete-filled steel tubes (CCFT or RCFT). The cross-sectional specimens were subjected to simulations that first applied an axial load and then monotonically increased the bending moments while holding the axial load constant. The simulations utilized fiber models consisting of steel and concrete two-dimensional fiber elements available in OPENSEES (Mazzoni et al., 2005). Simulations included both monotonic and cyclic analyses. The mid-height moment-curvature response ($M-\phi$) of CFT specimens was extracted in order to estimate the overall rotational capacity of composite CFT

beam-columns. The initial P-M interaction curves were formulated using monotonic fiber analyses. These studies verified that the simplified P-M interaction formulas from *2005 AISC Specification* are able to accurately predict the capacity of the CFT beam-columns. In the second part of these analyses, the envelopes of the cyclic moment-curvature responses generated from the fiber models were compared and calibrated with those of monotonic moment-curvature response. Finally, the cyclic results were used to determine the available curvature ductility ratios for these members (Varma et al., 2004), and these ratios were used to assess the performance of composite frames that undergo considerable deformations.

The assessment methods implemented for composite CFT beam-columns as described above can be extended to composite frame analyses. Within these frame analyses, both static pushover and linear and non-linear dynamic time history analysis were performed on simplified two dimensional moment resisting frames. Two primary indices were used to quantify expected performance. The first, which was used for the static and linear dynamic analysis, will be labeled the elastic strength ratio (ESR) and compares the bending plus axial load ratio generated from the frame analyses to that provided by the section selected in the design process. The second, which will be used for the non-linear dynamic analysis, is the inelastic curvature ductility ratio (ICDR) and compares the required rotational ductility given by the frame analysis with the yield ductility predicted by the cross-section one. In addition, both total roof and inter-story drifts were used to investigate frame performance.

3. Overview of applicable 2005 AISC Specification and 2005 Seismic Provisions

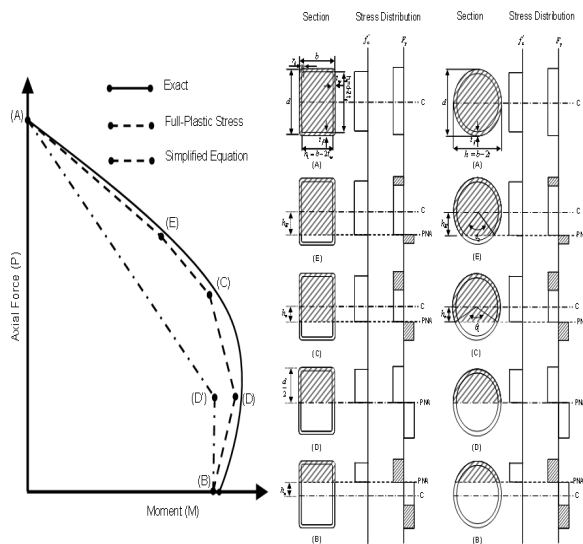
The current *2005 AISC Specification* (AISC Specification, 2005) includes design guidelines for composite columns consisting of rolled or built-up structural steel shapes, pipe or Hollow Steel Section (HSS) and structural concrete component acting together as a composite member. To qualify as a concrete filled composite column, the following requirements should be satisfied:

- The cross sectional area of HSS shall be at least 1 percent of the total composite cross section.
- The maximum width-thickness ratio for a rectangular

HSS shall be less than or equal to $2.26 \sqrt{E/F_y}$.

- The maximum diameter-thickness ratio for a circular HSS filled with concrete shall be equal to $0.15 E/F_y$.
- Larger slenderness are permitted when verified by either experimental tests or advanced analyses.

The 2005 AISC Specification endorses the use of the full plastic stress distribution to calculate cross-sectional strength. The calculations are based on the assumption of linear strain across the section height and perfectly elasto-plastic behavior. The nominal strength is estimated by assuming that the steel has reached its yield stress under either tension or compression and that the concrete has reached its crushing strength under only compression as shown in Fig. 1. The corresponding stress on an equivalent concrete stress block is taken as $0.85f'_c$ and $0.95f'_c$ for RCFTs and CCFTs, respectively.



(1) P-M interaction diagrams for composite beam-columns. (2) Full plastic stress distributions for RCFT and CCFT at point A,E,C,D and D.

Fig. 1 P-M interaction diagram for the composite CFT section and full plastic stress distribution over the section height at five specific points

The P-M interaction diagram (Fig. 1) for a composite section based on a full plastic stress distribution can be generated as a conservative linear interpolation between five points (Table 1) (19). Point (A) and Point (B) indicate the plastic axial strength and flexural strength of the section, respectively. Point (C) is anchored to the same flexural capacity as Point (B), but its axial

resistance comes from the concrete portion in compression only. Point (D) corresponds to the balanced failure condition, giving the maximum flexural strength for the section and an axial capacity equal to one half of that determined for Point (C). Point (E) is an additional, arbitrarily located point to better capture any bulges in the interaction diagram region corresponding to high axial loads. All five points are defined according to Table 1. For design, a simplified bilinear interpolation may be used between Point (A), (D') and (B) as also shown in Fig. 1. The simplified equations shown in Table 2 can be used for determining an index to use as the member capacity in the computation of the elastic strength ratios of composite beam-columns. This approach is reasonably accurate for steel columns and should provide a conservative estimate for composite structures. In so far as the frame designs are concerned, those are governed by the *Seismic Provisions* (Seismic Provisions, 2005) Four potential classes of Composite Moment Frame (C-MF) are identified in the Part II of the *Seismic Provisions* (Seismic Provisions, 2005) as shown in Table 3. For this study, composite special moment frames (C-SMF), the most ductile system, were selected for the design of several trial low-rise moment frames. Five-story buildings with long bays (36ft. or 11m) and perimeter moment resisting systems were used because the intent is to demonstrate the economy of this system for the market segment that constitutes about 90% of the steel frame construction in the USA. The buildings were designed to the loading prescribed by ASCE 7-05 (ASCE, 2002). The primary purpose of the ASCE 7-05 standard is to provide information useful to determine the required strength, interstory drift and seismic use group for a given structure type (SDC) assigned to a building is a classification based upon the occupancy class and the seismicity of the site. SDC A, B and C generally correspond to structures with the moderate seismic risk or low importance, while SDC D, E, and F require special seismic detailing in areas of high seismic risk or for critical structures. The designs herein satisfy all the requirements of C-SMF for SDC D.

4. CFT beam-column analyses

Two CFT relatively stocky cross sections were modeled as numerical fiber sections using OPENSEES program (Mazzoni et al, 2005) as shown in Fig. 2. The rectangular tube has a wall slenderness of 24.5, well below the limit of 56.7 allowed by the *Specification* ($F_y = 320$ Mpa or 46 ksi). Similarly, the circular tube has a slenderness of 36 well below the limit of 103.6 allowed by the *Specification* ($F_y = 290$ Mpa or 42 ksi).

The numerical CFT beam-column specimens are made up of flexible elements based on nonlinear stress-strain material response with discrete fiber sub-regions (e.g. quadrilateral, circular and triangular shapes). The monotonic analyses were carried out utilizing a uniaxial bilinear stress-strain behavior with small kinematic hardening for the steel tube and the uniaxial compressive Kent-Scott-Park stress-strain behavior model for confined concrete. The latter includes a degrading linear unloading / reloading stiffness.

Table 1. P-M interaction strength formulas for five specific points

Point	Equation for RCFT	Equation for CCFT
(A)	$P_A = A_s F_y + A_c (0.85 f'_c)$ $M_A = 0$ $A_s = \text{area of steel shape}$ $A_c = h_1 h_2 - 0.858 r_i^2$	$P_A = A_s F_y + 0.85 f'_c A_c^*$ $M_A = 0$ $A_s = \pi r_m t$ $P_A = A_s F_y + 0.95 f'_c A_c \text{ (Loaded in only axial compression)}$ $r_m = \frac{d-t}{2}$ $A_c = \frac{\pi h^2}{4}$
(E)	$P_E = \frac{1}{2} (0.85 f'_c) A_c + 0.85 f'_c h_1 h_2 + 4 F_y t_w h_E$ $M_E = M_{\max} - \Delta M_E$ $Z_{sE} = b h_E^2 - Z_{cE} \quad Z_{cE} = h_1 h_E^2$ $\Delta M_E = Z_{sE} F_y + \frac{1}{2} Z_{cE} (0.85 f'_c)$ $h_E = \frac{h_n}{2} + \frac{d}{4}$	$P_E = (0.85 f'_c A_c + F_y A_s) - \frac{1}{2} \left[F_y (d^2 - h^2) + \frac{1}{2} (0.85 f'_c) h^2 \right] \left[\frac{\theta_2}{2} - \sin \frac{\theta_2}{2} \right]$ $M_E = Z_{sE} F_y + \frac{1}{2} Z_{cE} (0.85 f'_c)$ $h_E = \frac{h_n}{2} + \frac{d}{4}$ $Z_{sE} = \frac{d^3 \sin^3 \left(\frac{\theta_2}{2} \right)}{6} - Z_{cE} \quad Z_{cE} = \frac{h^3 \sin^3 \left(\frac{\theta_2}{2} \right)}{6}$ $\theta_2 = \pi - 2 \arcsin \left(\frac{2 h_E}{h} \right)$
(C)	$P_C = A_c (0.85 f'_c)$ $M_C = M_B$	$P_C = 0.85 f'_c A_c \quad P_B = 0$ $M_C = M_B \quad M_B = Z_{sB} F_y - \frac{1}{2} Z_{cB} (0.85 f'_c)$
(D)	$P_D = \frac{0.85 f'_c A_c}{2}$ $M_D = Z_s F_y + \frac{1}{2} Z_c (0.85 f'_c)$ $Z_s = \text{full y-axis plastic section modulus of steel shape}$ $Z_c = \frac{h_1 h_2^2}{4} - 0.192 r_i^3$	$P_D = \frac{0.85 f'_c A_c}{2}$ $M_D = Z_s F_y + \frac{1}{2} Z_c (0.85 f'_c)$ $Z_s = \text{plastic section modulus of steel shape} = \frac{d}{6} - Z_c$ $Z_c = \frac{h^3}{6}$
(B)	$P_B = 0$ $M_B = M_D - Z_{sn} F_y - \frac{1}{2} Z_{cn} (0.85 f'_c)$ $Z_{sn} = 2 t_w h_n^2$ $Z_{cn} = h_1 h_n^2$ $h_n = \frac{0.85 f'_c A_c}{2 [0.85 f'_c h_1 + 4 t_w F_y]} \leq \frac{h_2}{2}$	$P_B = 0$ $M_B = Z_{sB} F_y - \frac{1}{2} Z_{cB} (0.85 f'_c)$ $Z_{sB} = \frac{d^3 \sin^3 \left(\frac{\theta_1}{2} \right)}{6} - Z_{cB} \quad K_c = f'_c h^2$ $K_s = F_y r_m t$ $Z_{cB} = \frac{h^3 \sin^3 \left(\frac{\theta_1}{2} \right)}{6} \quad h_n = \frac{h}{2} \sin \left(\frac{\pi - \theta}{2} \right) \leq \frac{h}{2}$ $\theta_1 = \frac{0.0260 K_c - 2 K_s}{0.0848 K_c} + \frac{\sqrt{(0.0260 K_c + 2 K_s)^2 + 0.857 K_c K_s}}{0.0848 K_c}$

Table 2. Simplified 2005 AISC Equations for stress ratios

Prior condition	Simplified equation
$P_r < P_D$	$\frac{M_r}{M_B} < 1$
$P_r \geq P_D$	$\frac{P_r - P_D}{P_A - P_D} + \frac{M_r}{M_{D'}} \leq 1$

Table 3. The summarize table for C-MF structures

The type of C-MF	Main deformation/yield shape	A total inter-story drift angle	SDC	Special system requirements
C-PRMF	Limited yielding in column base Main yielding in the ductile components	0.04 radian	C or below	A nominal strength is at least equal to 50 percent of M_p
C-SMF	Main yielding in the beams Limited inelastic deformations in the columns and/or connections	0.04 radian	D and above	The required strength shall be determined with the flexural strength (LRFD: $R_y M_n$)
C-IMF	Main yielding in the beams Moderate inelastic deformations in the columns and/or connections	0.03 radian	C and below	-
C-OMF	The limited inelastic action will occur in the beam, columns and/or connections	-	A and B	-

For the cyclic simulations, the stress-strain behavior of the steel fibers includes the effects of isotropic strain hardening, local buckling and biaxial stress. The cyclic stress-strain model for the concrete fibers includes the effects of stress degradation and crack opening and closing.

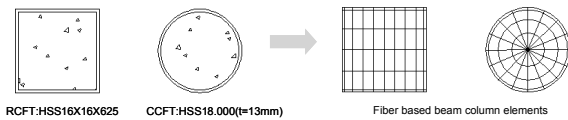


Fig. 2 Cross sections for Composite CFT and idealized fiber section models for numerical experiments (Use $F_y = 345 MPa$ and $f'_c MPa$)

The numerical test setup for a fiber based nonlinear beam-column element is shown in Fig. 3. The test model was subjected to various levels for the axial force, roughly corresponding to the axial load levels of the five interpolation points given by the code provisions. The axial load as applied first and then the moment was increased. Both element deformations and forces were recorded at each integration point. These integration points can be converted into simple zero-length section elements to represent the force-deformation relationship (P_e and $M-\phi$) for the crosssection (Mazzoni et al., 2005; Varma et al.,

2004). This section element is defined by the two nodes at the same position and discrete fiber based section shown in Fig. 3.

Typical results for the CFT beam-columns are shown in Fig. 4 for case where these elements are subjected to monotonic and cyclic eccentric load. The latter is composed of a fixed axial load corresponding to the axial resistance from half of the pure concrete part (P_D or Point D in Fig. 1) and increasing bending moment. In later comparisons, an Elastic Strength Ratio (ESR) will be computed by substituting the maximum monotonic flexural strength (M_u) from Fig. 4 for the required strength (M_r) in the formulas shown in Table 2. Note again that the Equations in Table 2 imply a relationship for design of the type shown by line A-D'-B in Fig. 1.

The Bauschinger effect, and gradual strength and stiffness degradation can be observed in the cyclic moment-curvature behavior in Fig. 4. However, since the material properties are assumed as ductile and the material strains are not capped, these models show excellent performance. Envelopes of the cyclic moment-curvature response of inelastic section element are also shown in Fig. 4. This envelope is used to determine the ultimate moment capacity (M_u), the

initial flexural stiffness (K_i) and the Inelastic Curvature Ductility Ratios (ICDR). K_i is defined as the initial secant stiffness corresponding to the serviceability level of moment (taken as $0.6M_u$). ICDR are defined as ϕ_u divided by ϕ_y . ϕ_y indicates the curvature at nominal yield, defined as M_u divided by K_i . ϕ_u is the ultimate curvature generally corresponding to the 90 percent of M_u , as a measure of post-peak behavior. This percentage is arbitrary and can change according to the amount of strength degradation and the type of loading.

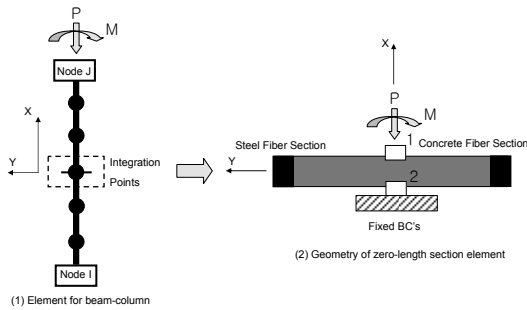


Fig. 3 Nonlinear beam-column element and zero-length section element

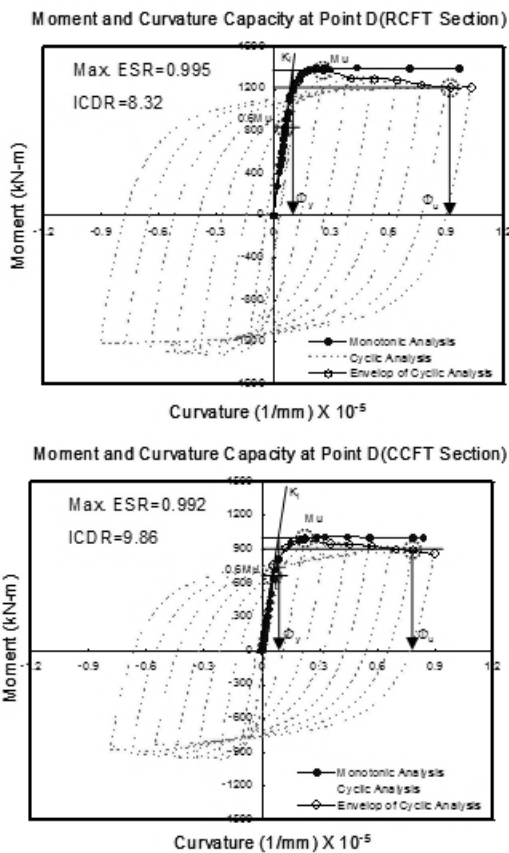


Fig. 4 Moment and curvature responses for composite CFT sections under the axial force P_D

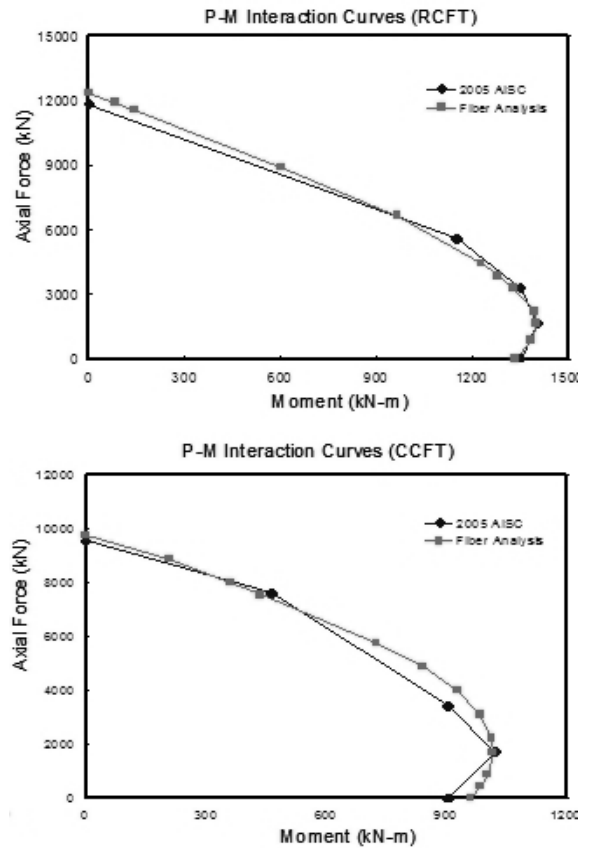


Fig. 5 Comparisons of P-M interaction strength between 2005 AISC code provisions and fiber analysis result

Comparisons of P-M interaction strength as predicted by the OpenSEES analyses and the simplified equations in the 2005 AISC Specification are shown in Fig. 5. The OpenSEES results are shown for a point which corresponds to the achievement of the maximum concrete strength in the Kent-Scott-Park model. The results in Fig. 5. show the accuracy of the 2005 AISC Specification in evaluating the capacity of the composite CFT structures.

5. Moment resisting frame analyses

The two dimensional composite moment resisting frames designed for this study were first evaluated using an equivalent static lateral load procedure (pushover) and then using both linear and non-linear dynamic analysis for a ground motion taken from the 1994 Northridge earthquake. For the non-linear dynamic analysis, geometric non-linearities were included in the formulation. The equivalent lateral

loads (E_a) used in the static analysis (Fig. 6) are based upon the code-calculated period of vibration (0.79 sec.) and not the actual ones (1.28 sec. for the RCFT structure and 1.25 for the CCFT one). This moment frame was assumed to be located in a high seismic area corresponding to SDC D and a hard rock site (ASCE, 2002). The frame was designed as a composite special moment frame (C-SMF) for ordinary occupancy and a target story drift limit of 0.02 radians for the 2 percent probability of exceedance in 50 year seismic hazard level. The frame was detailed in accordance with Section 10 of the 2005 *Seismic Provisions*, and overall dimensions and member sizes are shown in Fig. 7. The design of this frame was governed by drift considerations, resulting in members with a substantial overstrength compared to that required from the strength design case. This is typical of moment frames designed in areas of high seismicity by USA codes.

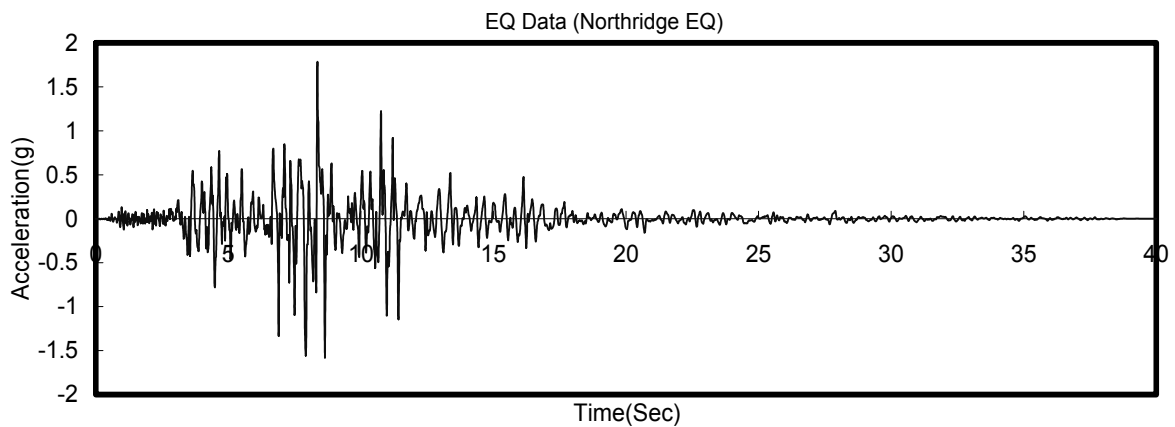
For the static analyses, factored dead loads and live loads along with the earthquake loads (Fig. 6(a)) were applied at the joints using the load combination $1.2D+0.5L+1.0E_a$. For the dynamic analyses, the

unscaled EW base accelerations from the Tarzana station (Fig. 6(b)) recorded during the 1994 Northridge were used. The PGA for this record is 1.78g and this ground motion includes strong directional effects. In the non-linear analyses, a dead load factor of 1.0 and live load factor of 0.5 were used to provide a realistic gravity loading.

The numerical experiments were performed by the OPENSEES program with all members modeled as nonlinear beam-column elements with discrete fiber sections. Fixed joint conditions were assumed at all connections. All analyses utilized the Newton-Raphson iteration algorithm to ensure equilibrium at each time step. Static analyses were conducted using load a control method, while dynamic analysis was performed by implicit integration using the Newmark-Beta constant acceleration method. For the dynamic analysis, the structural damping ratio was assumed to be 0.025 and the equivalent point masses were applied at the joints. Fig. 8 shows a comparison of the three types of analyses, while Fig. 9 shows the results of the pushover analysis normalized by the design base shear (V_{design}) and yield displacement (Δ_y).

Story	Dead Load (D)	Live Load (L)	Lateral Load (RCFT, E_a)	Lateral Load (CCFT, E_a)
5	4.79 kPa	3.83 kPa	213kN	178kN
4	4.79 kPa	3.83 kPa	377kN	314kN
3	4.79 kPa	3.83 kPa	450kN	375kN
2	4.79 kPa	3.83 kPa	417kN	348kN
1	4.79 kPa	3.83 kPa	269kN	224kN

(1) Static loads



(2) The pseudo- dynamic load

Fig. 6 Equivalent static loads and pseudo-dynamic load

From the frame analyses, Elastic Strength Ratios (ESR) and Inelastic Curvature Demand Ration (ICDR) for all the CFT columns were obtained. Maximum values for ESR and ICDR for the RCFT and CCFT frame structure are shown on Fig. 10 and Fig. 11 respectively.

The maximum ESR under equivalent static loads can not exceed 1.0 because these frame structures satisfied the design code requirements. A symbol “-” in Figs. 10 and 11 indicates that the member force did not exceed the yield point.

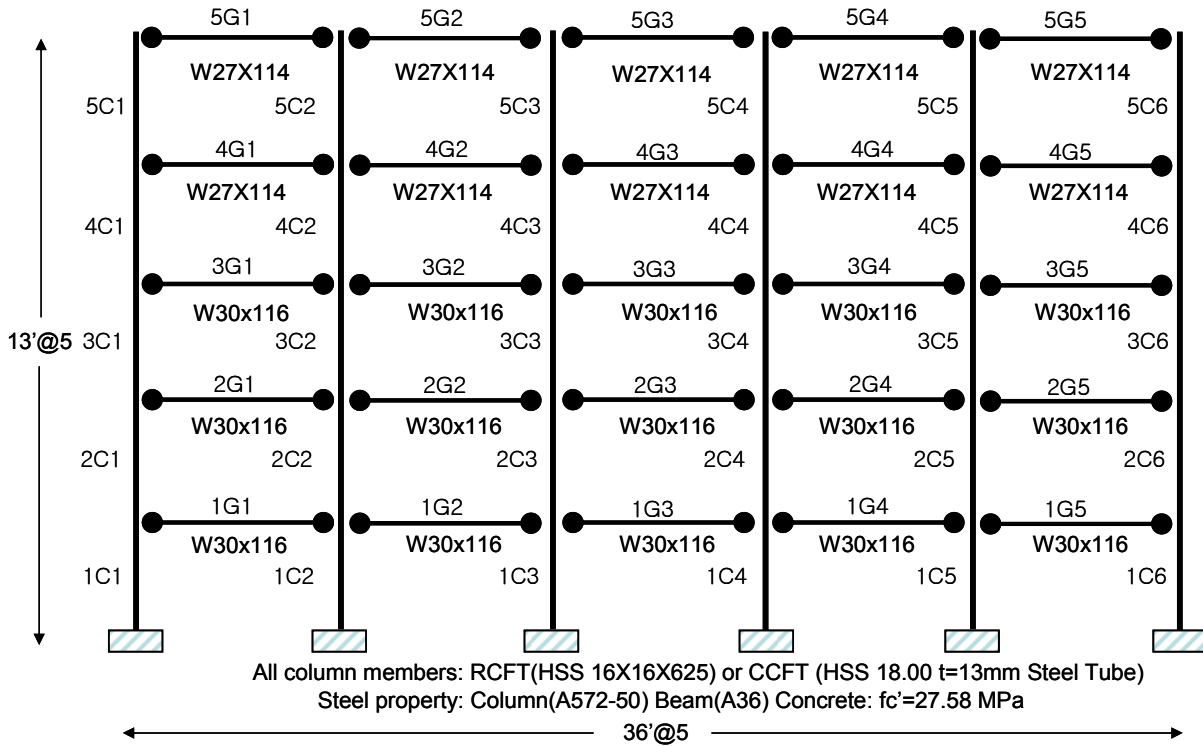


Fig. 7 The 5 story composite moment frame structure-a typical front view

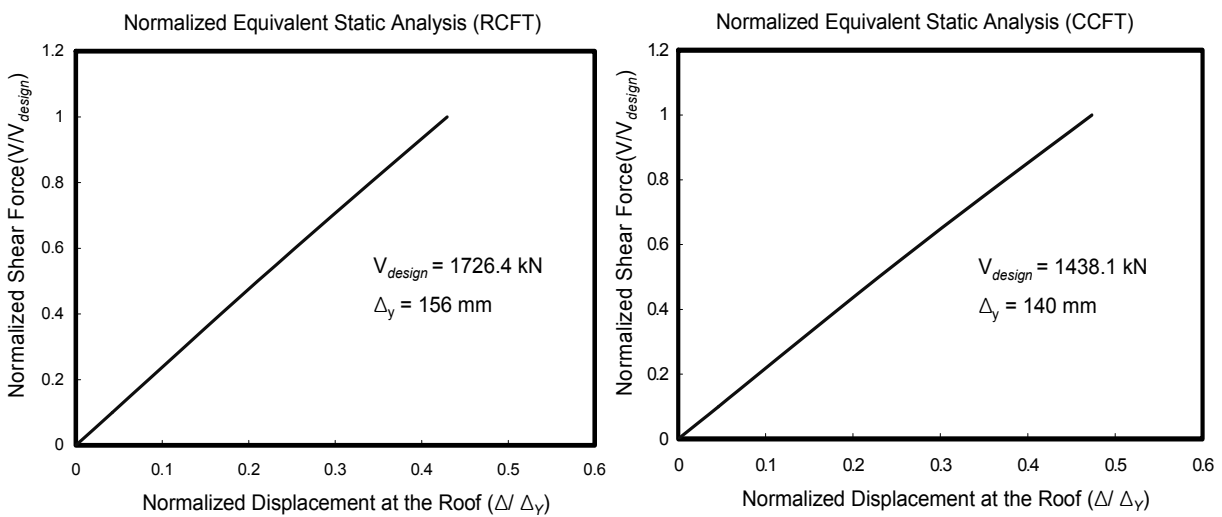


Fig. 8 (a) Normalized elastic equivalent static analysis

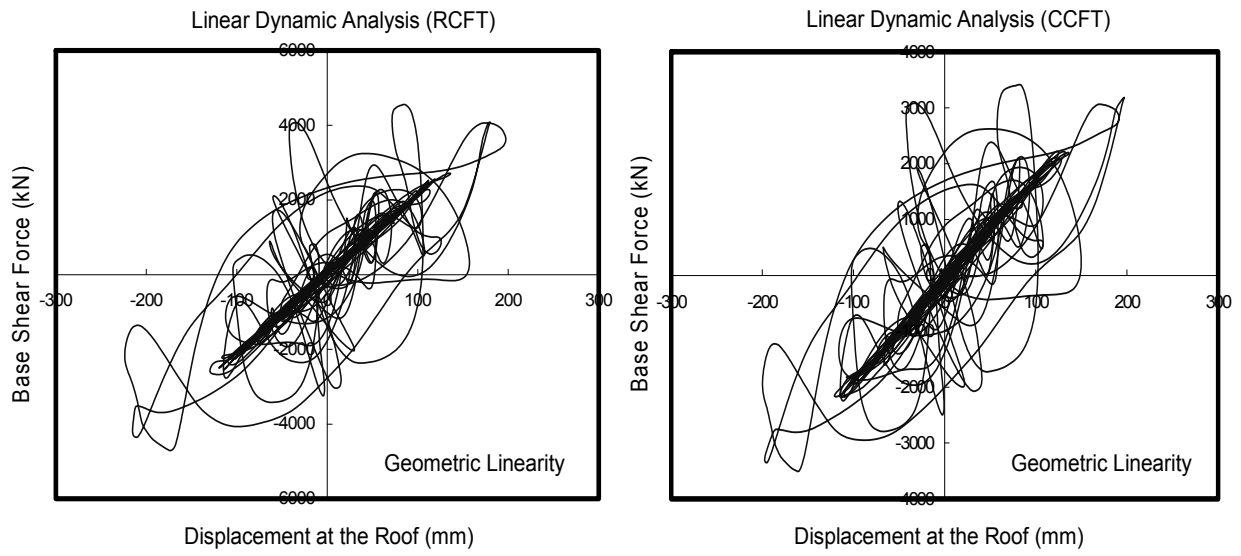


Fig. 8 (b) Linear dynamic analysis

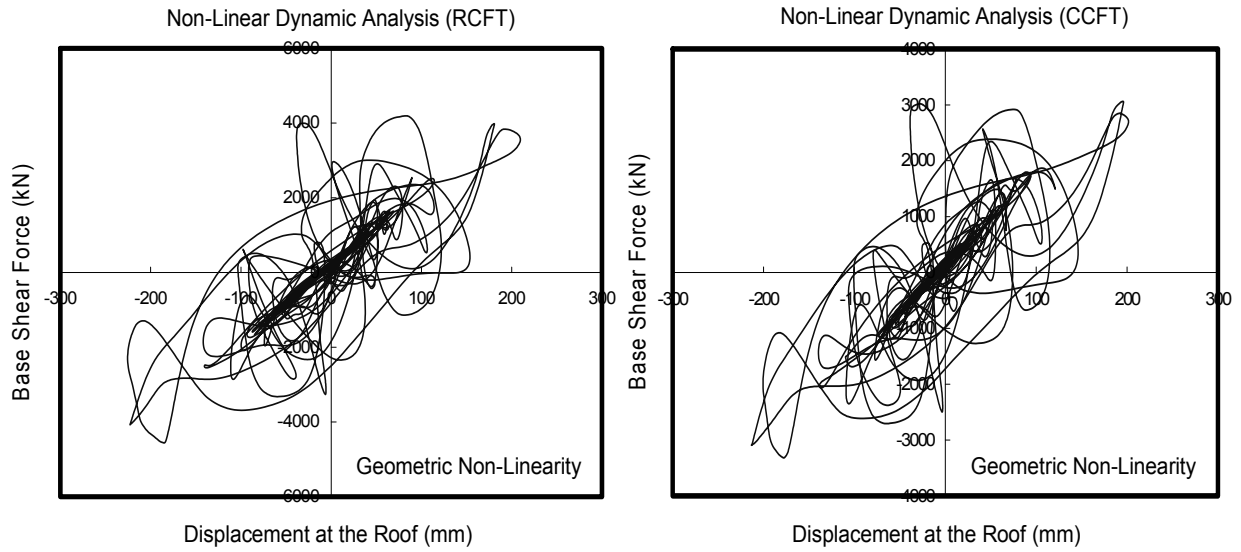


Fig. 8 (c) Nonlinear dynamic analysis

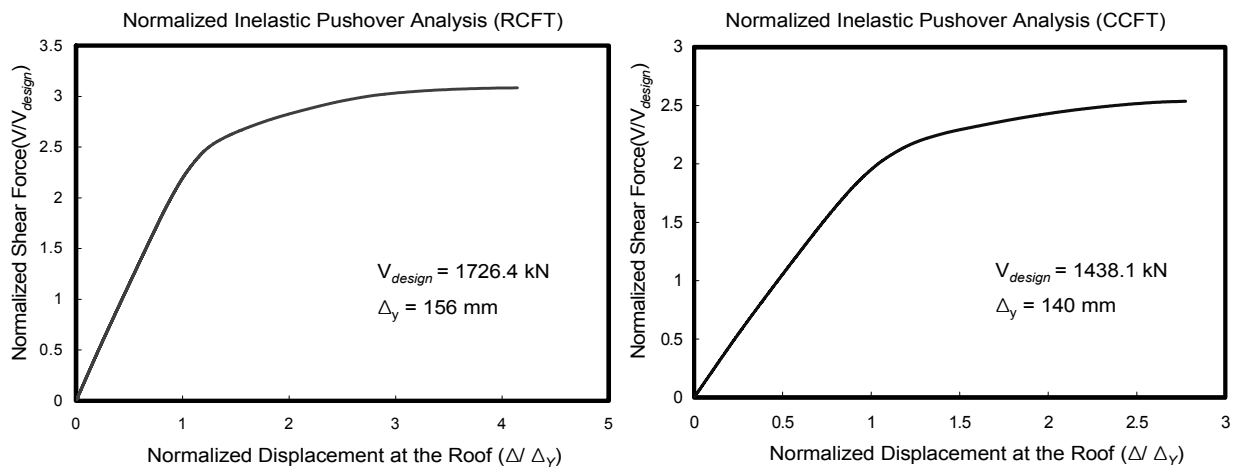
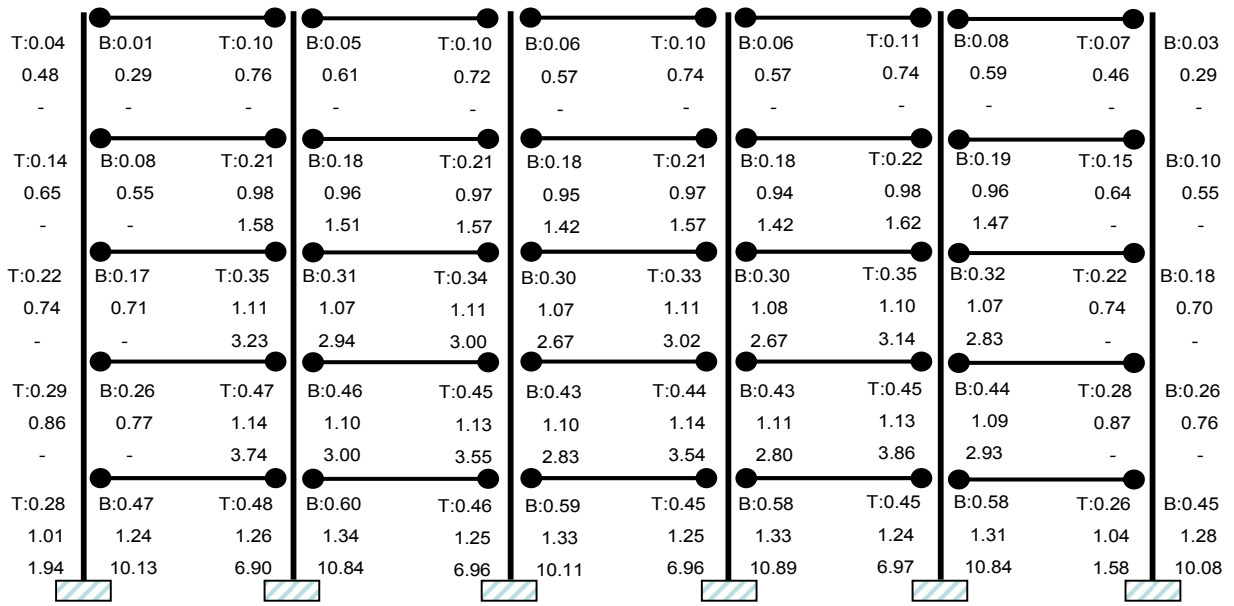
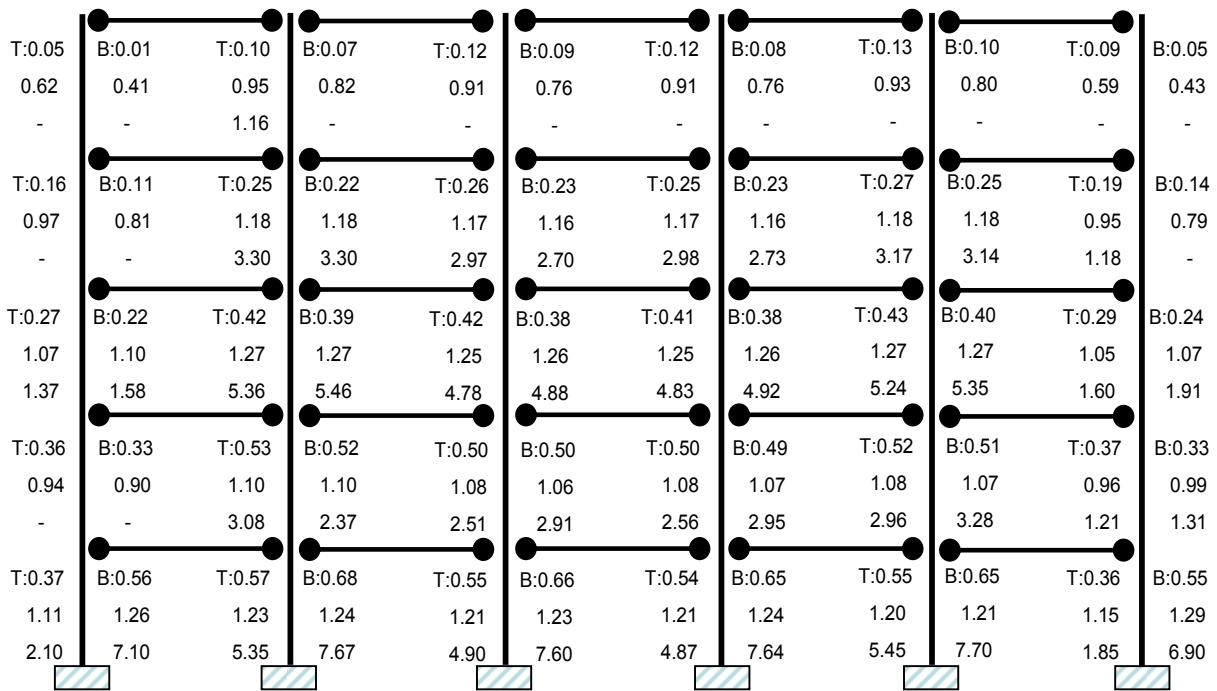


Fig. 9 Normalized inelastic pushover analysis



- (1) Equivalent static analysis (Max. ESR) T: The top of a RCFT member
- (2) Pseudo-dynamic analysis (Max. ESR) B: The bottom of a RCFT member
- (3) Pseudo-dynamic analysis (ICDR)

Fig. 10 Max. ESR and ICDR for C-MF with RCFT columns



- (1) Equivalent static analysis (Max. ESR) T: The top of a CCFT member
- (2) Pseudo-dynamic analysis (Max. ESR) B: The bottom of a CCFT member
- (3) Pseudo-dynamic analysis (ICDR)

Fig. 11 Max. ESR and ICDR for C-MF with CCFT columns

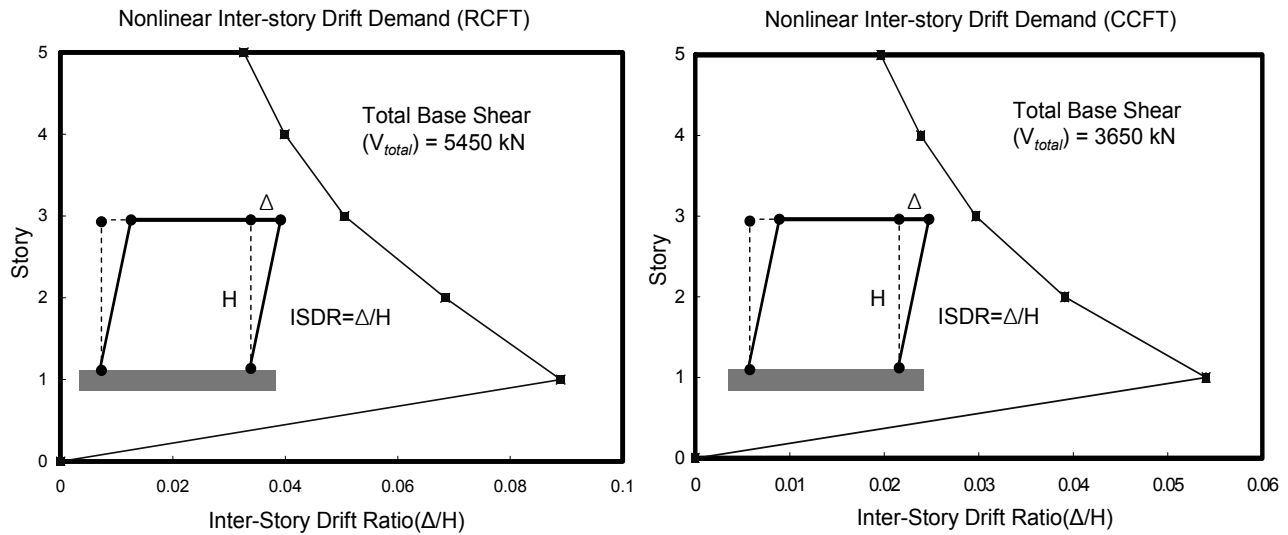


Fig. 12 Nonlinear inter-story drift ratios

An ESR of over 0.95 under dynamic loads indicates that the observed member exceeded its yield point and will potentially be subject to a large ductility demand.

As seen in the figures, the ESR resulting from the static analysis using equivalent lateral loads are considerably smaller than those resulting from the linear dynamic analysis using site ground motions. For the critical interior columns in the first story, the ratio of the elastic pushover ESR to the linear dynamic ESR can be very high (3.1 and 2.6 for the top and bottom of column 1C3 in Fig. 8). This implies that the design is unconservative, as extensive member failures and overall frame damage can occur due to the actual seismic ground motion. The maximum ICDR and ESR generally occur at the interior column of first floor (1C2, 1C3, 1C4 and 1C5). This indicates that the interior columns at the first floor have a great possibility to undergo large deformation. Inter-Story Drift Ratios (ISDR) obtained by the nonlinear pushover analysis prove this argument as shown in Fig. 12.

6. Conclusion and Design Recommendation

The new 2005 AISC Specification was used to estimate P-M interaction diagrams for composite CFT beam-columns and the 2005 Seismic Provisions were used for the design of several low-rise composite moment frame structures. The comparisons between fiber analysis results obtained by numerical experiments and

interaction diagrams obtained by AISC design formulas indicate that full plastic capacities by this new design code are quite reasonable for predicting the interaction strength for composite beam-columns. The cyclic analysis for CFT specimens shows gradual strength/stiffness degradation, elastic unloading and Bauschinger effect due to the cyclic stress-strain behavior of steel and concrete fibers. For the composite frame analyses, ESR from elastic analyses and ICDR from inelastic analyses show significant correlation with predicted damage based on excessive deformation. Similar numerical distribution trends between ESR and ICDR are observed in both RCFT frame and CCFT frame structures and larger values are found in interior CFT columns of the lower floors when structure models are subjected to either static or dynamic loading. Higher equivalent lateral loads occur at the mid-floors of composite moment frame structures. ESR and ICDR decrease moderately with increasing building story, so damage in the upper floor columns is not expected. For both frame models, the dynamic analysis can produce maximum ESR which are quite higher than the static analysis values. The frame structures under seismic loads have to dissipate the total seismic energy in order to decrease structural damage. Finally, it can be verified through ISDR that the interior columns at the first story level contains large deformation under excessive lateral loads.

Acknowledgments

This research was supported by Basic Science Research Program through the National Research Foundation of Korea (NRF) funded by the Ministry of Education, Science and Technology (Grant No. 2012R1A1A1041521). The authors gratefully acknowledge this support.

References

- AISC Specification (2005). "Specification for Structural Steel Buildings." (*ANSI/AISC 360-05*), Chicago
- ASCE (2002). "Minimum Design Loads for Buildings and Other Structures." *ASCE 7-05*, USA.
- Azizinamini, A. and Schneider, S. P. (2001). "Moment Connections to Circular Concrete-Filled Steel Tube Columns." *J. Struc. Eng., ASCE*, 130(2), pp. 213-222.
- Deierlein, G. G. (1998). "Summary of SAC Case Study Building Analysis." *J. Perform. Construc. Facil., ASCE*, 12(4), pp 202-212.
- El-Tawil, S., Kanno, R., and Deierlein, G. G. (1996). "Inelastic Models for Composite Moment Connections in RCS Frames, Composite Construction in Steel and Concrete III." ASCE Special Publication, Edited by Buckner, C. D and Shahrooz, B., SEI, *American Society of Civil Engineers*, pp. 197-210.
- FEMA (1995). "NEHRP Recommended Provisions for Seismic Regulations for New Buildings and Other Structures, Part 1 and 2, 1994 ed., Report FEMA 222A and 223A." *Federal Emergency Management Agency*, Washington, D.C., USA.
- Galambos, T. V. (ed.) (1998). *Guide to Stability Design Criteria for Steel Structures*. Structural Stability Research Council, 5th edition, John Wiley and Sons, NewYork, NY.
- Green, T. P., Leon, R. T. and Rassati, G. A. (2004). "Bidirectional Tests on Partially Restrained, Composite Beam-Column Connections." *J. Struc. Eng., ASCE*, 130(2), pp 320-327.
- Hajjar, J. F. et. al. (1998). "Analysis of Mid-Rise Steel Frame Damaged in Northridge Earthquake." *J. Perform. Construc. Facil., ASCE*, 12(4), pp 221-231.
- Hajjar, J. F. (2002). "Composite steel and concrete structural systems for seismic engineering." *J. Construc. Steel Res.* 58, pp 703-723
- Kim, D. K. (2005). *A Database for Composite Columns, Master Thesis in School of Civil and Environmental Engineering*. Georgia Institute of Technology, Gerogia, USA.
- Mazzoni, S., Mckenna, F., Fenves, G. L. (2005). *Opensees Command Language Manual*. Department of Civil Environmental Engineering, University of California, Berkley, CA, USA.
- Rassati, G. A., Leon, R. T. and Noe, S. (2004). "Component Modeling of Partially Restrained Composite Joints under Cyclic and Dynamic Loading." *J. Struc. Eng., ASCE*. 130(2), pp 343-351.
- Roeder, C. W. (2000). "Seismic Behavior of Steel Braced Frame Connections to Composite Columns." *Connections in Steel Structure 4* (R. Leon and S. Easterling, eds.), AISC, pp. 51-62.
- Seismic Provision (2005). "Seismic Provisions for Structural Steel Buildings." *ANSI/AISC 341-05*, Chicago, USA.
- Seon, W. H. and Hu, J. W. (2011). "Continuum Based Plasticity Models for Cubic Symmetry Lattice Materials Under Multi-Surface Loading." *J. Korean Soc. Adv. Comp. Struc.*, 2(3), pp. 1-11.
- Tsai, K. C. et al. (2004). "Pseudo Dynamic Tests of a Full-Scale CFT/BRB Composite Frame." *Proc. of the 2004 Structure Congress, ASCE*.
- Varma, A. H. et. al. (2004). "Seismic Behavior and Design of High-Strength Square Concrete-Filled Steel Tube Beam Columns." *J. Struc. Eng., ASCE*, 130(2), pp. 169-179.
- Viest, I. M. et al. (1997). *Composite Construction Design for Building*. Co-published by ASCE, McGraw-Hill, Chapter 5.3., USA.